Astronomy & Astrophysics manuscript no. proj1
November 21, 2019

Stellar parameters determination

Project I - Computational Astronomy

Rui Peixoto

Departamento de Física e Astronomia, Faculdade de Ciências, Universidade do Porto

November 21, 2019

ABSTRACT

Aims. A systematic and efficient method to determine stellar parameters from observed spectra by comparison with synthetic spectra is developed and implemented.
Methods. Stellar parameters are estimated and observed spectra are compared with preselected synthetic spectra by equivalent width comparison of select fitted spectral lines. Selected synthetic spectra are then processed and interpolated to facilitate comparison with observed spectra.
Results. Computational method is implemented and two stars analysed. Sensibility to a stars' high rotational velocity, effects of experimental noise, good fit conditions are discussed and pathological cases analysed.

1. Introduction

Spectral analysis is a fundamental tool in astronomy and astrophysics. A good understanding of spectra is a key factor not only to observational astronomy, but also to the understanding of phenomena best displayed in astronomical context, such as high-energy physics, plasma physics and cosmology.

In this context, a systematical analysis of spectra potentiates the value of forthcoming increases in instrumental resolution for accurately determining stellar parameters. The exercise of developing sensible computational methods here employed is therefore a worthwhile endeavor.

2. Spectra Comparison

From the comparison of observed with synthetic spectra one may conclude much about the observed object. While a direct comparison (using a least squares fit method, for example) is possible, it is not the most efficient or insightful approach. To take advantage of refined (and consequently large) synthetic spectra databases, one must explore more efficient ways of comparing spectra. With this goal, we compare instead the equivalent width, W, of known FeI spectral lines (in this case, Tsantaki et al. (2013)).

This method of comparison naturally avoids most of the effects of noise inherent to observed spectra, due to the way of calculating W, while simultaneously providing a considerable speedup.

3. Method

3.1. Equivalent width and Gaussian fit

At the core of the method is the idea that the equivalent width of a spectral line may be estimated by employing a Gaussian fit (Figure 1) and computing (Monteiro & Gameiro (2019)).

$$W_0 = \int_{\lambda_0-k}^{\lambda_0+k} \frac{F_{\text{cont}} - F_{\text{line}}}{F_{\text{cont}}} \tag{1}$$

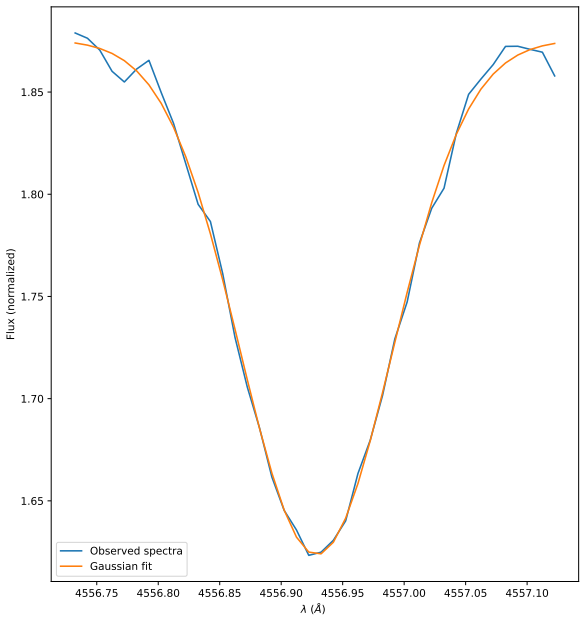

Fig. 1. Gaussian fit to spectral line

where F_{cont} is the continuum line and k some appropriate limitation such that a line is isolated but not cut. Computationally, the integral need not be computed, as one can get the width from the Gaussian parameters only, by setting F_{cont} as the additive parameter of the fit.

3.2. Temperature estimation

With efficiency in mind, we start by estimating the effective temperature of our spectra, as this allows us to limit the range of

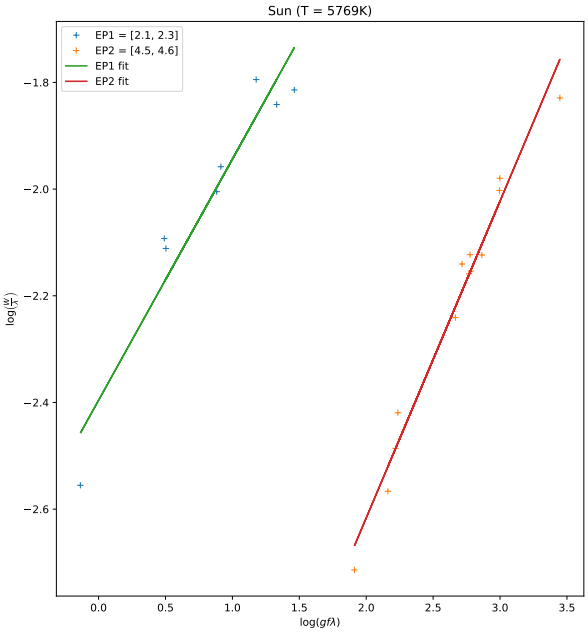

Fig. 2. Sun's temperature estimation

spectra to lookup in the database greatly. We achieve this by calculating the equivalent width of lines of two multiplets of sufficiently different excitation energy and plotting $log\,(W/\lambda)$ by $\log\,(gf\lambda)$. From the relation (Monteiro & Gameiro (2019))

$$\log\left(\frac{W_\lambda}{\lambda}\right) = \alpha + \log\,(\lambda f_i g_i) - \frac{5040}{T_{\rm exc}}\chi_i \tag{2}$$

with $\log\,(\lambda f_i g_i)$ and χ_i know for each multiplet (Tsantaki et al. (2013)), and α a constant, we may denote the average distance between linear fits (for which equation 2 is common) as Δ and obtain

$$T_{\rm exc} = \frac{|5040\,(\chi_2 - \chi_1|)}{\Delta} \tag{3}$$

Using known equivalent widths for the sun's lines (Figure 2) we get $T = 5769$ K directly from equation 3.

3.3. Synthetic spectra database lookup and comparison

Setting an uncertainty interval on the temperature ΔT (in our case, $\Delta T = 400$K), one may now compare the observed spectra with synthetic spectra (in Laverny et al. (2012)) with temperatures in the range $T \in [T - \Delta T, T + \Delta T]$.

This comparison proceeds once again by calculating the equivalent width of known lines of both spectra. We may then plot $W_{\rm synt}$ by $W_{\rm obs}$ and determine the best synthetic spectra by determining the one corresponding to a linear fit of slope closest to unity. [1]

[1] Alternatively, a least squares comparison may be used. The reasons for not using this method will be clarified later. They may nevertheless be reduced to equivalent methods, depending on the choice of lines. Due to the efficiency of computational fitting methods, there is no significant slowdown.

3.4. Synthetic spectra processing

With the best fitting spectra found, one need only process it before the comparison with the observed spectra. This consists of:

1. applying the experimental profile of the instrument of measurement used, by means of a convolution of the spectra with a Gaussian determined by the experimental parameters as in equation 4 (Monteiro & Gameiro (2019)).

$$\sigma = \frac{<\lambda>}{R\sqrt{8\ln(2)}} \tag{4}$$

   being σ the standard deviation of the Gaussian function and R the resolution of the instrument ($R \approx 50000$ for HARPS used in Tsantaki et al. (2013)).
2. applying the rotational profile of the star by #TODO
3. interpolating the synthetic spectra with observed data for ease of posterior analysis.

4. Conclusions

1. The conditions for the stability of static, radiative layers in gas spheres, as described by Baker's (**?**) standard one-zone model, can be expressed as stability equations of state. These stability equations of state depend only on the local thermodynamic state of the layer.
2. If the constitutive relations – equations of state and Rosseland mean opacities – are specified, the stability equations of state can be evaluated without specifying properties of the layer.
3. For solar composition gas the κ-mechanism is working in the regions of the ice and dust features in the opacities, the H_2 dissociation and the combined H, first He ionization zone, as indicated by vibrational instability. These regions of instability are much larger in extent and degree of instability than the second He ionization zone that drives the Cepheïd pulsations.

Acknowledgements. Part of this work was supported by the German *Deutsche Forschungsgemeinschaft, DFG* project number Ts 17/2–1.

References

Laverny, P. d., Recio-Blanco, A., Worley, C. C., & Plez, B. 2012, Astronomy & Astrophysics, 544, A126
Monteiro, M. J. & Gameiro, J. 2019, Sebenta UC Astronomia Computacional
Tsantaki, M., Sousa, S. G., Adibekyan, V. Z., et al. 2013, Astronomy & Astrophysics, 555, A150